Driving Sustainable Energy Dispatch for Remote Communities Using Levy Flight Salp Swarm Algorithm

Benjamin O. Ajayi, Anthony Ibe, Boniface A. Oriji, Toyin O. Odutola

Emerald Energy Institute, University of Port Harcourt, Nigeria

DOI: https://doi.org/10.51244/IJRSI.2024.1108096

Received: 08 August 2024; Accepted: 13 August 2024; Published: 15 September 2024

ABSTRACT

This study evaluates three energy dispatch algorithms to find the best way to improve hybrid energy systems in rural areas: load following (LF), cycle charging (CC), and a novel customized strategy (CS). The study examined solar and wind resources as well as projected patterns of energy consumption with a particular focus on Bambur village in Taraba State, Nigeria. The Levy Flight Salp Swarm Algorithm (LFSSA) was used in the study to assess system configurations for each method, accounting for battery storage, wind turbines, diesel generators, and photovoltaic (PV) arrays. The most cost-effective and efficient approach was determined to be the Customized Strategy (CS), which produced the lowest Net Present Cost (NPC) of $1,959,100 and Levelized Cost of Energy (LCOE) of $0.119/kWh. The Load Following (LF) technique had the highest costs at $2,204,736.10 and $0.134/kWh, while the Cycle Charging (CC) method had intermediate costs with an NPC of $2,083,770 and an LCOE of $0.127/kWh. With a 580-kWh battery bank, a 10 kW wind turbine, 332 kW of PV capacity, and a 78 kW diesel generator, the CS approach showed better component sizing balance. The trade-offs between energy output, storage, and backup power in real-time were optimized using this design. Sensitivity analysis revealed that increasing interest rates from 10% to 18% led to a rise in LCOE, while diesel cost fluctuations showed a non-monotonic impact on LCOE, peaking at $0.79/L before declining due to increased reliance on renewable sources and storage. CS strategy's balance of investment and efficiency makes it ideal for remote energy management, offering key insights for rural electrification.

Keywords: Hybrid Energy System (HES), Dispatch Strategies, Levelized Cost of Energy (LCOE), Net Present Cost (NPC), Levy Flight Salp Swarm Algorithm (LFSSA)

INTRODUCTION

Nigeria's rich cultural diversity and natural resources are overshadowed by challenges like rural electricity shortages and the need for sustainable development. These issues, critical to national development, impede daily life and economic growth. Many rural areas lack reliable electricity, affecting education, healthcare, and industries, thereby perpetuating poverty and underdevelopment [1].

The critical need for power generation based on renewable energy (RE) to meet future energy issues is highlighted by the world's rapidly diminishing fossil fuel sources. The use of fossil fuels increases emissions significantly, underscoring the need of using renewable energy sources like wind and solar power. Hybrid energy systems (HES) have made it feasible and efficient to integrate these dispersed renewable energy sources [2].

Stand-alone HES can be a useful option for decentralized power generation and distribution in remote locations, especially when combined with diesel backup. Renewable energy sources like wind and solar power are especially useful in this regard. By utilizing the plentiful and sustainable energy derived from natural sources, these systems lessen dependency on fossil fuels and encourage environmental sustainability [1], [2], [3], [4], [5], [6], [7], [8], [9], [10]. Rural areas face challenges such as poor road access, isolated locations, and high supply costs, making grid extension impractical. Diesel generators are often used but come with high costs, maintenance needs, and pollution [11]. Nigeria's ample renewable resources—solar and wind—offer an alternative. Studies advocate for solar PV, wind, and hybrid systems to provide sustainable and efficient power

[1], [2], [3], [4], [5], [6], [7], [8], [9], [10]. Successful dispatch strategies are essential for optimizing these systems, reducing costs, and enhancing reliability [12], [13], [14].

Energy control strategies in hybrid energy systems optimize resource utilization, reduce costs, and enhance reliability. They improve efficiency, extend component lifespans, and promote environmental sustainability. These strategies drive technological advancements, making renewable energy more viable and encouraging wider adoption of hybrid systems. Cycle Charging (CC) maximizes battery use by charging during low demand or high renewable generation and discharging during peaks, increasing renewable energy use and efficiency. Load Following (LF) dynamically adjusts power generation to demand changes, optimizing renewables and grid stability.

Several studies have compared different dispatch strategies, some with grid connections and others with standalone grids. These studies examined existing strategies like LF and CC, along with other dispatch strategies [2], [4], [5], [6], [7], [8], [9], [10], [15], [16], [17], [18]

Most papers focused on performance parameters such as NPC and COE [2], [4], [5], [6], [7], [8], [9], [10], [15], [16], [17], [18], while some included CO2 emissions as a performance parameter [2], [7], [9], [15], [17], [19]

This study introduces a Customized Strategy (CS) that combines the benefits of LF and CC by optimizing battery charging and discharging based on projected load demands and anticipated renewable energy generation. A planned PV/Wind/Diesel/Battery HES designed to electrify the off-grid rural area of Bambur, Taraba State, Northern Nigeria, is analyzed, which was developed in MATLAB. The approach uses the Levy Flight Salp Swarm Algorithm (LFSSA) to determine which of the three dispatch strategies—LF, CC, and CS—is the best. This algorithm's main goal is to maximize the share of renewable energy while lowering the Levelized Cost of Energy (LCOE) and Net Present Cost (NPC).

METHODOLOGY

This section presents the methodological framework for developing and optimizing the HES, starting with mathematical models of energy sources. This is followed by the description of the study area.

A. Energy Source Modeling

Mathematical modeling is vital for designing, optimizing, and assessing hybrid energy systems. It helps predict power flow, determine optimal component sizes, and integrate solar, wind, and storage technologies, ensuring efficient, reliable, and economically viable systems. This approach advances sustainable energy by enhancing system performance and grid integration.

1) PV system modelling:

Solar irradiance, or the quantity of sun exposure, and local temperature are two important factors that impact the performance of a photovoltaic (PV) system. The formula given illustrates how to calculate the power generated by the photovoltaic system (PPV) [17] in Equation (1).

$$P_{PV} = Y_{PV} f_{PV} \left(\frac{G_T}{G_{T,ST}}\right) \left[1 + \alpha_P \left(\frac{T_C}{T_{C,ST}}\right)\right] \qquad (1)$$

In this equation:

Y_{PV}: Represents PV array's rated capacity in kilowatts (kW).

f_{PV}: PV derating factor, expressed as a percentage.

G_T: Shows the kW/m2 of the solar radiation that is currently reaching the PV array.

$G_{T,ST}$: indicates incident radiation in accordance with standards conditions (ST), typically set at 1 kW/m2.

T_C: current PV cell temperature in °C.

αP: Indicates the temperature coefficient of power, expressed as a percentage change per degree Celsius (°C).

T_C, ST: PV cell temperature under ST.

2) Wind turbine modelling:

Utilizing wind power, wind turbines generate electricity. Their power production is strongly influenced by the wind speed. As wind speeds fluctuate at different heights, observed wind speeds usually need to be modified to account for the precise working height (hub height) of a wind turbine. The hourly power generation of the wind turbine is calculated using Equation 2 [20].

$$P_{WDT}(t) = \begin{cases} 0 & \text{if } v_{\text{hub}} < v_{\text{cut-in}} \text{ or } v_{\text{hub}} \geq v_{\text{cut-out}} \\ P_{WDT\_r}\left(\frac{v_{\text{hub}}^3}{v_R^3 - v_{\text{cut-in}}^3}\right) - P_{WDT\_r}\left(\frac{v_{\text{cut-in}}^3}{v_R^3 - v_{\text{cut-in}}^3}\right) & \text{if } v_{\text{cut-in}} \leq v_{\text{hub}} < v_r \\ P_{WDT\_r} & \text{if } v_r \leq v_{\text{hub}}(t) < v_{\text{cut-out}} \end{cases} \quad \ldots(2)$$

Two wind speeds are taken into account in the equation: V_hub(t), which is the wind speed (m/s) at the hub height (h_hub) (meters) of the wind turbine, and V_ref(t), which is the reference wind speed (m/s) recorded at the height (H_ref) (meters) of the anemometer. The friction coefficient is represented by the symbol α.

Equation 3, which describes the wind profile power law, is a well-known equation that we can use to achieve this conversion [21]:

$$\boldsymbol{V_{hub}}(t) = \boldsymbol{V_{ref}}(t)\left(\frac{\boldsymbol{h_{hub}}}{\boldsymbol{h_{ref}}}\right)^{a} \qquad (3)$$

3) Battery Storage System Modeling:

Battery storage is essential for HES to operate because it stores extra energy during high-generation periods and generates power during low-output periods. Equation (4) for the energy state at each point of charging at time t was presented by [22].

$$\begin{aligned} \boldsymbol{E_{BSS}(t) = E_{BSS}(t-1)(1-\sigma) + E_{excess}\,\eta_{BSS}} \\ \boldsymbol{E_{BSS}(t) = E_{BSS}(t-1)(1-\sigma) - E_{deficit}} \end{aligned} \qquad \textbf{(4)}$$

- σ: Battery self-discharge rate.
- E_{excess}: Excess energy stored in the battery.
- η_{BSS}: Battery charging efficiency.
- $E_{deficit}$: Deficit energy

4) State of Charge (SOC):

“A battery's operating mode is primarily influenced by its State of Charge (SOC), which indicates the present charge level compared to its maximum capacity. SOC is essentially the opposite of Depth of Discharge (DOD), defined by the equation SOC = 1 – DOD, as presented by Equation (5)” [22]).

$$SOC(t) = SOC(t-1) + \frac{\Sigma N_i P_i(t) - P_{\text{load}}(t)}{V_{BSS} C_{BSS}} \qquad (5)$$

Ni: Number of generator units (i).

$P_{i(t)}$: Generator (i) power output at time t.

$P_{load(t)}$: The load's power requirement at time t.

V_{BSS}: Voltage of the battery.

C_{BSS}: Battery capacity.

5) Diesel Generator Modeling:

When the energy requirements of the system cannot be satisfied by the combined energy provided by the solar panels, wind turbines, and battery storage, DG is employed as a backup power source in HES. [23] propose a method to calculate the DG's fuel usage and its associated cost (CfDG) using:

$$C_{f\_DG} = \alpha_{DG} \times P_{DG}(t) + \beta_{DG} \times P_{\text{rated\_DG}} \qquad (6)$$

C_{f_DG}: Fuel consumption of the DG.

$P_{DG(t)}$: The average power supplied by the DG at time t.

P_{rated_DG}: The DG's rated power output capacity.

α_{DG} and β_{DG}: Consumption coefficient curve values specific to the DG, representing different operating conditions. This study used for this case, αDG = 0.246 and βDG = 0.08145 l/kWh [18].

6) Rectifier Model:

Rectifier provides a steady DC voltage to charge the battery storage system (BSS) from the AC power produced by the diesel engine. This conversion is performed during the CC dispatch is in play. The energy that is used to power the BSS ($P_{Rect\_o}(t)$) can be estimated using the following equation (Eq. 7):

$$P_{Rect\_o}(t) = P_{Rect\_i}(t) \times \eta_{Rect} \quad (7)$$

Where $P_{Rect_i}(t)$ is the amount of power that the rectifier receives from the AC source, and η_{Rect} is the power rectifier's efficiency.

7) Inverter Model:

Equation 8 can be used to calculate $P_{Invt\_o}(t)$ which is the rectifier's contribution to the battery storage system (BSS) charging process from the diesel engine's AC power [22]:

$$P_{Invt\_o}(t) = P_{Invt\_i}(t) \times \eta_{Invt} \quad (8)$$

Where $P_{Invt\_i}(t)$ is the amount of power that comes from the DC source to the inverter, and η_{Invt} signifies the power inverter's efficiency.

B. Optimization Problem Formulation

The dispatch strategy outlines the necessary operations for generators and storage units in the event that renewable resources are not sufficient to meet load demand. The suggested approach combines the benefits of CC and LF to maximize the use of renewable energy sources [22].

With this method, battery charging decisions are made in accordance with projected load demands and energy output from renewable sources. It can be difficult to operate every HES component efficiently. Thus, for a

ISSN No. 2321-2705 | DOI: 10.51244/IJRSI |Volume XI Issue VIII August 2024

dependable and economical system, proper energy management is crucial in addition to component sizing. The study prioritizes RE sources above battery storage (BS), with the diesel engine only turning on when both sources are unable to meet the load requirements.

Mode 1: Excess Energy and Battery Charging

The battery storage absorbs the excess power if the total energy supplied by RESs at a given time interval (net load < 0) and the battery state of charge is lower than its maximum.

Mode 2: Excess energy supplied to dump loads

With SOC at maximum, surplus energy is sent to dummy loads to prevent overcharging and prolong battery life if the total energy from RESs surpasses the load demand.

Mode 3: Perfect Match

The overall energy output from renewable energy sources exactly meets the load demand when the net load is zero. This balance ensures that energy production and consumption are perfectly aligned, eliminating the need for additional energy from the battery or any supplementary sources.

Mode 4: Maintaining Power Balance with Battery Storage

If the SOC is higher than the minimum threshold (SOC > 30%) and the RESs are insufficient to meet the load requirement (net load > 0), the energy shortage is provided by the stored energy in the battery.

Mode 5: DG is used to fill the net load gap when energy from renewable sources and energy stored in battery banks are not enough to meet the load requirement.

1) Objective Function: The objective of this research is to identify the ideal component sizes for a hybrid energy system (HES) in order to reduce LCOE. This guarantees a consistent supply of electricity at a more affordable price. Equation (9) is used to determine LCOE, which is the average cost per kWh of energy produced over the system's lifetime. This allows for a consistent comparison of various configurations, taking into account salvage value, replacement costs, operating, and maintenance expenses.

$$LCOE = \frac{(C_{INT}+C_{OM}+C_{REP}-S_{SAL})*CRF}{\sum_{t=1}^{8760} E_{gen}(t)} \quad (9)$$

$$CRF = \frac{r(1+r)^n}{(1+r)^n-1} \quad (10)$$

Where:

C_{INT} - initial capital cost of component

CRF - Capital Recovery Factor

C_{OM} - annual operation and maintenance cost

C_{REP} - annual replacement cost

S_{SAL} - salvage value

E_{gen} - energy production

r - discount rate

ISSN No. 2321-2705 | DOI: 10.51244/IJRSI |Volume XI Issue VIII August 2024

2) Annualized Capital Cost: Annualized Capital Cost represents the yearly portion of initial investments in equipment and infrastructure, spread over their useful lifespan (Eq 11). It is calculated by spreading initial investment costs over the system's lifetime, using an appropriate discount rate for annual payments.

$$C_{INT} = \sum_{j=1}^{N} C_{INTj} \qquad (11)$$

Where C_{INTj} - for component j of the system.

3) Operations and Maintenance Cost (C_{OM}): C_{OM} covers the routine expenses necessary to keep the hybrid energy system running efficiently and reliably. It is determined by estimating yearly expenses required for system upkeep, including labor, repairs, and regular maintenance activities (Eq. 12).

$$C_{OM} = \sum_{j=1}^{N} C_{OMj} \qquad (12)$$

4) Replacement Cost: Equation (13), which represents replacement cost, takes into account the money needed to replace system components that have reached the end of their useful lives. It is assessed by forecasting the cost of replacing components as they reach the end of their useful life within the system.

$$C_{REP} = \sum_{j=1}^{N} \frac{C_{REPj}}{(1+r)^{t_i}} \qquad (13)$$

C_{REPj} is the cost of replacing component *j*.

5) Salvage Value: It is the amount of the system's components' residual worth that can be obtained through recycling or resale when its useful life is coming to an end. It is estimated based on the residual value of components at the end of their lifespan, considering resale or recycling possibilities.

$$C_{SAL} = \sum_{j=1}^{N} C_{INTj} X (1 - \frac{t_{sys}}{L_i}) \qquad (14)$$

C_{INTj} is the initial cost of component *j*.

t_{sys} *is the entire operational lifetime of the system.*

L_i *is the expected lifespan of component* j.

C. Modelling of HES

This research introduces a novel energy dispatch strategy named the Customized Strategy (CS) for optimizing power dispatch in hybrid energy systems. The CS prioritizes renewable energy sources by leveraging the strengths and mitigating the weaknesses of two existing strategies: LF and CC.

The study uses LFSSA to optimize the system setup using the MATLAB simulation tool. Comparison is made between the results of different energy dispatch systems, such as LF, CC, and Customized Strategy (CS). In order to minimize the system's COE and NPC while maintaining adherence to predetermined operational limits, the ideal number of photovoltaic (PV) modules, wind turbines, battery banks, and diesel generator capacity must be determined.

Customized Strategy (CS) offers superior performance over cycle charging (CC) and load following (LF) by dynamically adapting to changing conditions. It uses intelligent prediction and state of charge (SOC) feedback to optimize fuel economy and battery sustainability. Unlike static CC, which lacks adaptability, and LF, which doesn't optimize for efficiency, CS handles the complexities of hybrid energy systems more effectively by balancing load demands and renewable variability.

ISSN No. 2321-2705 | DOI: 10.51244/IJRSI |Volume XI Issue VIII August 2024

D. Hybrid Energy System Components

The analysis assumes a system lifetime of 20 years, and the system components (PV modules, wind turbines, diesel generator, and battery storage) are defined in Table 3.1.

Specification of the system components

Solar PV	
Capital cost	1300$/kW
Replacement cost	1050$/kW
O&M Cost	5$/yr
Lifetime	25year
Efficiency	20%

Wind turbine	
Initial cost per unit	5100$/kW
Replacement cost	5450$/kW
O&M Cost	50$/yr
Hub height	24m
Lifetime	20year

Hydrogen Tank	
Capital cost	410$/kg
O&M Cost	4.1$/kg/year
Lifetime	20year

Battery Storage	
Capacity	1kWh
Initial cost per unit	310$/kW
Replacement cost	255$/kW
O&M Cost	5$/yr
Maximum Depth of Discharge	20
Throughput	800

Converter	
Capital cost	302$/kW
Replacement cost	255$/kW
O&M Cost	5$/yr
Lifetime	15year
Inverter Efficiency	95%
Rectifier Efficiency	95%

Diesel Generator	
Initial cost per unit	200$/kW
Replacement cost	195$/kW
O&M Cost	0.05$/yr
Lifetime	15000hours
Conversion Efficiency	30%
Diesel price	1.8$/L
Fuel curve slope	0.236L/hr/kW

Fuel Cell	
Capital cost	3000$/kW
Replacement cost	2700$/kW
O&M Cost	0.025$/kW/h
Lifetime	20year

Electrolyte	
Capital cost	2000$/kW
Replacement cost	1800$/kW
O&M Cost	20$/kW/year
Lifetime	15

Table I - The System Components

E. Optimization Techniques

The Flight Levy Salp Swarm Algorithm (FLSSA) a novel optimization technique that combines the concepts of Lévy flight and the Salp Swarm Algorithm (SSA) is employed for the studies.

SSA is a cutting-edge optimization method modeled after nature that mimics the swarming behavior of salps in the ocean. The key aspects of the SSA are:

1. Initialization: As shown in Equation (15), the method begins by initializing the salp positions within the search space boundaries at random.

2. Salp Categorization: A leader and followers comprise the salp population. The swarm is directed toward the food source (optimal solution) by the leader salp.

3. Position Update: The leader's position is adjusted, as in Equation (16), based on random coefficients that balance exploration and exploitation and the current location of the food supply.

The followers' positions are updated according to the location of their previous salp using Newton's law of motion.

4. Fitness Evaluation: The fitness (objective function value) of each salp position is evaluated.

5. Iteration: Steps 3–4 are repeated until the termination criteria (such as the maximum number of iterations) are met.

The goal of the SSA is to replicate the coordinated and cooperative movement of actual salp swarms in the water in order to effectively search the search space and converge to the global optimum. When compared to other metaheuristic approaches, the algorithm's performance on a variety of optimization problems has shown promise.

$$X_p = \begin{bmatrix} x_1^1 & x_2^1 & \dots & x_d^1 \\ x_1^2 & x_2^2 & \dots & x_d^2 \\ . & . & \vdots & . \\ . & . & \dots & . \\ . & . & \dots & . \\ x_1^n & x_2^n & \dots & x_d^n \end{bmatrix} \qquad (15)$$

$$x_i^1 = \begin{cases} z_1 + a_1\left((ub_p - lb_p)a_2 + \ lb_p\right) & a_3 \geq 0 \\ z_1 + a_1\left((ub_p - lb_p)a_2 + \ lb_p\right) & a_3 < 0 \end{cases} \quad (16)$$

SSA uses the following parameters to navigate the search space:

- x_p^1 represents the first salp's location in the *pth* dimension.
- z_p represents the position of the food source in the *pth* dimension.
- lb_p and ub_p denote the lower and upper bounds of the *pth* dimension, respectively.
- a_1 is calculated using Eq. (17).
- a_2 and a_3 are random numbers between 0 and 1.

These parameters are used to guide the salps in their search for the optimal solution.

$$a_1 = 2\, e^{-\left(\frac{4l}{L}\right)} \quad (17)$$

A maximum of L iterations—where l is the current iteration—can be completed using this process.

The position of the follower is then updated using Newton's law of motion.

$$\boldsymbol{x_p^j} = \frac{1}{2}\boldsymbol{\lambda}t^2 + \boldsymbol{\delta_o}t \quad (18)$$

Within the optimization process, where each iteration acts as a unit of time (i ≥ 2), the follower salp's position ($\boldsymbol{x_p^j}$) is updated using its initial speed of zero ($v_o = O$) and its previous position. A coefficient (k) is defined as the final velocity divided by the initial velocity ($k = \frac{v_{final}}{v_o}$). Equation (31) then represents the updated position using this coefficient and the difference between the current and previous positions.

$$x_p^j = \frac{1}{2}(x_p^j + x_p^{j-1}) \quad (19)$$

This equation below helps identify salps that fall outside the designated search area.

$$x_p^j = \begin{cases} l^j & if\ \boldsymbol{x_i^j} \leq l^j \\ u^j & if\ \boldsymbol{x_i^j} \leq u^j \\ x_p^j & otherwise \end{cases} \quad (20)$$

The FLSSA leverages the Levy flight strategy along with the swarming characteristic of salps to enhance both exploration and exploitation in the search space. The algorithm divides the salp population into leaders and followers, with the leader leading the swarm and the followers trailing behind. The leader's position is updated using an algorithm that accounts for the location of the food source, search space limitations, and random factors. The followers' positions are updated using Newton's law of motion. The Levy flight strategy introduces long jumps that help the algorithm escape local optima. This approach balances exploration and exploitation, making it suitable for various optimization problems in engineering design, machine learning, and resource allocation.

Levy Flight Equation is given as

$$L(s) \sim \frac{1}{s^{1+\beta}} \quad (21)$$

ISSN No. 2321-2705 | DOI: 10.51244/IJRSI |Volume XI Issue VIII August 2024

$Where\ 1 < \beta \leq 3.$

$$x_{ij} = x_{ij} + \propto L(s) \qquad (22)$$

Where $\propto$ is a scaling factor, and L(s) is the step size generated from the Levy distribution in Equation 22.

Algorithm Steps

1. Set the salp population and settings to zero.
2. Assess each salp's fitness.
3. Update the leader's position using the leader update equation.
4. Update the followers' positions using Newton's law and incorporate Levy flight.
5. Check constraints and boundary conditions.
6. Until the stopping requirement is satisfied, repeat steps 2 through 5.

RESULT AND DISCUSSION

The outcomes of the estimated energy demand and renewable energy data for the study area are displayed in charts, followed by the use of LFSSA to compare various energy dispatch methods, such as Customized Strategy (CS), Cycle Charging (CC), and Load Following (LF).

A. Study Area and Population of the Study

The study examines the potential for renewable energy solutions in Bambur, a village situated in Taraba State, Nigeria. Bambur lies at approximately 9° 20' 59" North latitude and 11° 2' 41" East longitude. A part of Central Bambur is the area under study, encompasses roughly 200 residences, a primary healthcare center, a public primary school, and a bustling commercial hub.

Figure 1 - Location of the study area (Bambur)

The population is estimated at around 1,000, comprising regular dwellers and others who conduct business at the hub. The majority of the residents are engaged in agricultural activities. Similar to many villages in the region, Bambur currently lacks access to the national electricity grid.

The wind and sun irradiation data utilized in this study was obtained by the National Aeronautics and Space Administration (NASA). The estimated energy demand for Bambur were determined through a combined approach of data collection via questionnaires and subsequent validation by comparing the obtained data with the average energy demand of a typical village in Northern Nigeria. This multi-pronged approach ensured the accuracy and representativeness of the energy demand estimations for the village.

The average yearly solar radiation and wind speed, as determined by the study's analysis of 8760 hours of village data, are 5.61 kWh/m2/day and 5.12 m/s, respectively. The daily load demand curve for Bambur Village is shown in Figure 3.2. The average daily electrical load demand is 482 kWh, with an anticipated peak daily load demand of 26.75 kW. Energy use peaks twice daily: mornings **(5-8 AM)** and evenings **(7-10 PM)**, likely due to typical daily routines. To enable a comparative study of the patterns of energy consumption, the load demand is shown for the wet season and the dry season. The dry season experiences significantly higher demand, primarily driven by cooling needs and extended business hours compared to the wet season.

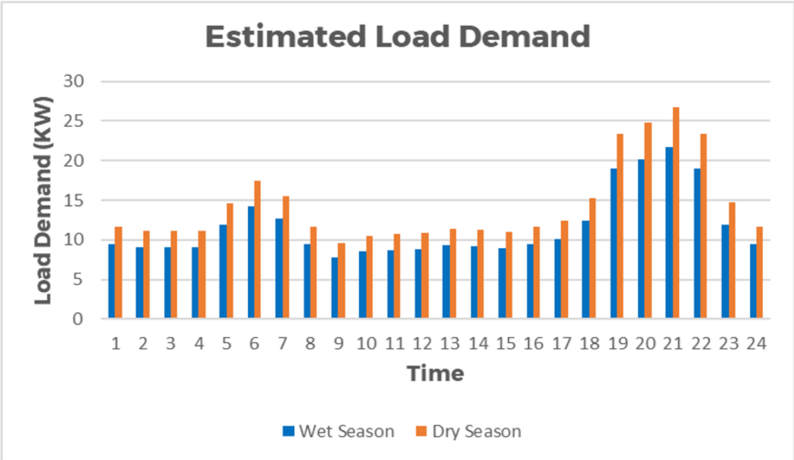

Figure 2 - Daily load demand in Bambur Village

B. Monthly wind speed in Bambur Village

Figure 3 highlights the wind speed data for Bambur, crucial for evaluating wind energy potential. Wind speeds peak at around 7 m/s in January and 6.5 m/s in December, indicating favorable conditions for wind energy generation. However, speeds drop to around 4 m/s in June and July, necessitating energy storage or additional sources to maintain a reliable energy supply.

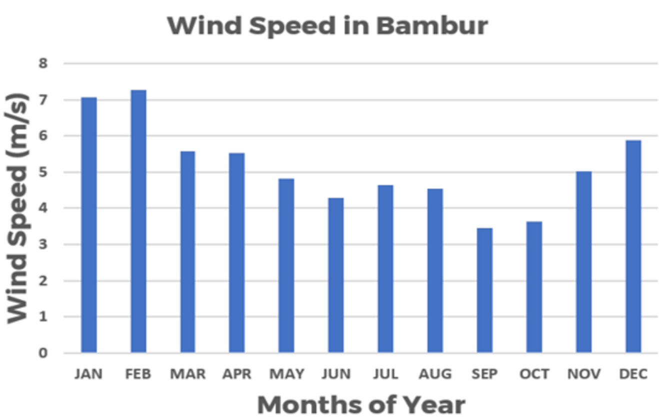

Figure 3 – Wind Speed in Bambur

C. Monthly solar radiation in Bambur Village

Figure 4 presents monthly solar radiation data for Bambur, crucial for assessing solar photovoltaic (PV) system performance. January and December show high solar radiation at around 5.7 kWh/m², and from February to April, levels remain consistently high at 5.9-6.5 kWh/m². May and June see a slight dip to about 5

ISSN No. 2321-2705 | DOI: 10.51244/IJRSI |Volume XI Issue VIII August 2024

kWh/m², while July and August exhibit the lowest levels at 4-4.5 kWh/m². Radiation increases again from September, peaking at 6.2 kWh/m² in November.

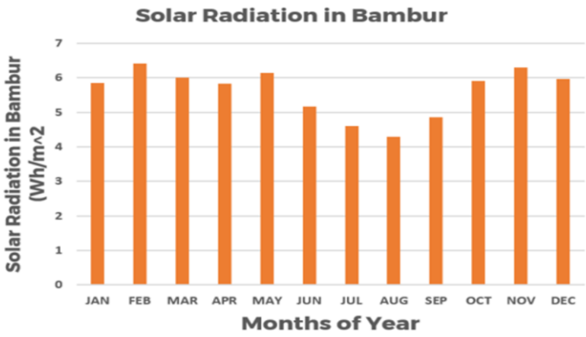

Figure 4 – Solar Radiation in Bambur

D. Hybrid Energy System

This analysis compares three strategies for a HES: LF, CC and CS. The components evaluated are Photovoltaic (PV) systems, Wind Turbines (WT), Battery Storage Systems (BSS), and Diesel Generators (DG) in Figure 5.

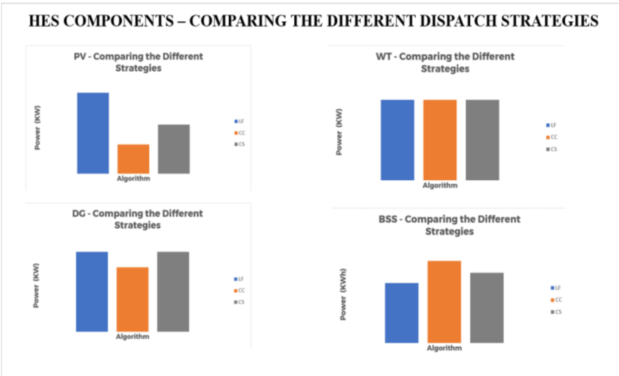

Figure 5 – Hybrid Energy System Components (PV, WT, DG & BSS)

1) Photovoltaic (PV) System: The Load Following strategy prioritizes real-time energy with 353 kW PV capacity. Cycle Charging, at 319 kW, relies more on storage and diesel. The Customized Strategy, with 332 kW, balances energy production and storage, aiming for cost efficiency and reliability.

2) Wind Turbine (WT): The consistent 10 kW wind turbine capacity across strategies suggests limited or consistent wind resources, making larger turbines unnecessary. Wind power plays a minor role compared to PV systems, and its integration isn't influenced by operational strategy choice.

3) Battery Storage System (BSS)

Energy dispatch strategies vary in battery capacities. Cycle Charging uses the largest at 679 kWh for maximum renewable utilization and minimal diesel use. Load Following, with 495 kWh, focuses on real-time generation. The Customized Strategy balances at 580 kWh, optimizing storage and costs.

4) Diesel Generator (DG): Generator size choices reveal distinct strategies: Load Following and Customized Strategy use a larger 78 kW generator for robust backup and grid stability during peaks. Cycle Charging, with a smaller 63 kW generator and larger battery, emphasizes stored renewable energy, reducing fossil fuel use and emissions.

5) Overall System Analysis: LF prioritizes immediate demand with the largest PV capacity and generator but smallest battery, leading to higher diesel use during low solar output. CC emphasizes storage with the largest battery but smallest PV and generator, minimizing diesel consumption. CS balances components, optimizing cost, reliability, and renewable use. All strategies reflect solar-driven systems with minor wind roles, highlighting location's solar potential and limited wind. Battery size variations emphasize storage's importance, and generator roles vary, demonstrating system flexibility for different operational goals.

E. HES with Relevant Parameters

This analysis examines the relevant parameters for the three strategies in a HES: LF, CC, and Customized Strategy (CS).

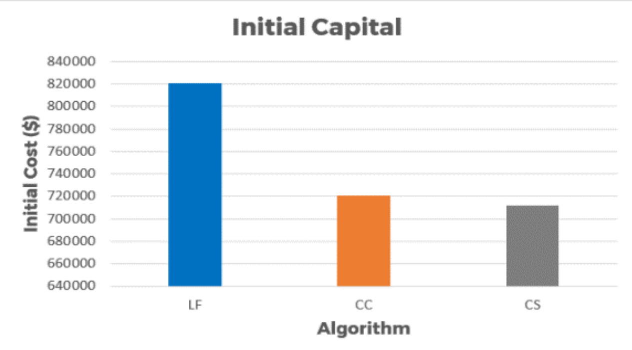

Figure 6 – Initial Capital Cost

1) Initial Capital Cost

The Customized Strategy (CS) has the lowest initial capital cost at $711,936.94, followed by Cycle Charging (CC) at $720,755.21 and Load Following (LF) at $821,043.72 as in *Figure 6*, CS system would require the least amount of upfront investment compared to the other two options.

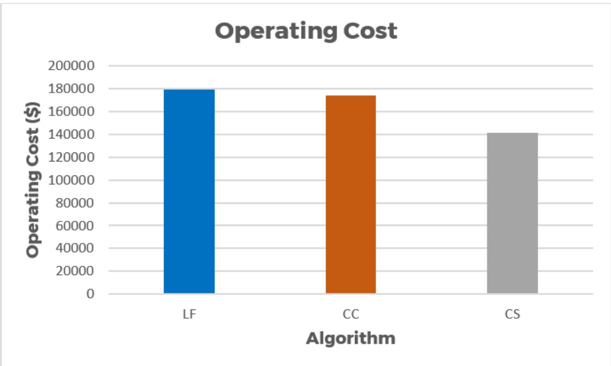

Figure 7 – Operating Costs

2) Operating Costs

Fig. 7 indicates the operating costs with Load Following (LF) has the highest at $179,588.98, followed by Cycle Charging (CC) at $173,903.11, while the Customized Strategy (CS) has the lowest at $141,340.45. Thus, CS is the most cost-effective option for operating expenses.

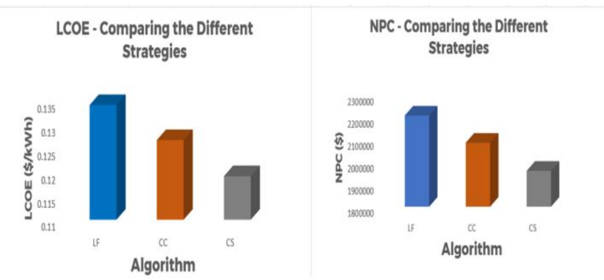

ISSN No. 2321-2705 | DOI: 10.51244/IJRSI |Volume XI Issue VIII August 2024

Figure 8 – LCOE and NPC – Dispatch Strategies (LF, CC & CS)

3) Net Present Cost (NPC):

Load Following (LF) has the highest NPC at $2,204,736.10 due to larger PV and diesel investments and higher operational costs. Cycle Charging (CC) has a moderate NPC of $2,083,770.00 (*Fig. 8*), balancing initial investments with efficient storage use. Customized Strategy (CS) has the lowest NPC at $1,959,100.00, optimizing costs and efficiency. These values indicate CS offers the best long-term economic performance, followed by CC, with LF incurring the highest costs.

4) Levelized Cost of Energy (LCOE):

Load Following (LF) has the highest LCOE at $0.134/kWh, indicating low cost-efficiency. Cycle Charging (CC) improves with $0.127/kWh, using energy storage efficiently. Customized Strategy (CS) achieves the lowest LCOE at $0.119/kWh, balancing renewables, storage, and backup. CS offers the most cost-effective energy production, followed by CC, with LF being the least economical.

5) CO_2 Emission

Figure 9 illustrates the carbon dioxide (CO2) emissions associated with three distinct algorithms: LF, CC, and CS, measured in kilograms per year. Among these, the CC algorithm exhibits the highest level of CO2 emissions, approximately 32,452 kg/year. Following closely, the LF algorithm generates emissions of 25,138 kg/year, while the CS algorithm records the lowest emissions, slightly below 24,897 kg/year.

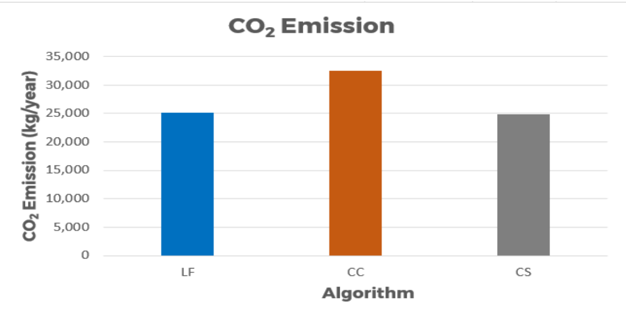

Figure 9 – CO_2 Emission

4) Overall System Analysis:

The Customized Strategy (CS) emerges as the most cost-effective option, featuring the lowest Net Present Cost (NPC) and Levelized Cost of Energy (LCOE), as well as the least CO2 emissions. Cycle Charging (CC) offers a lower-cost option compared to LF; however, it results in the highest CO2 emissions.

F. Sensitivity Test

The sensitivity analysis examines how variations in fuel prices and interest rates influence the LCOE and NPC.

ISSN No. 2321-2705 | DOI: 10.51244/IJRSI |Volume XI Issue VIII August 2024

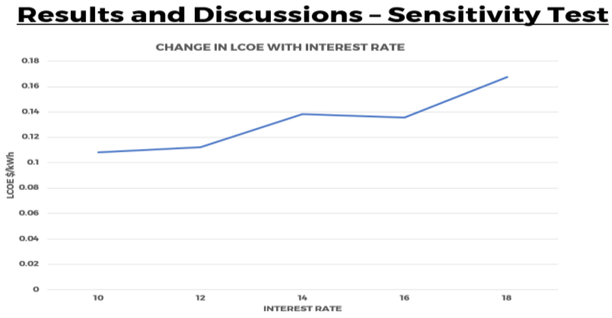

Figure 10 – Sensitivity with Interest Rate

Figure 10 illustrate the sensitivity analysis demonstrates that increasing interest rates from 10% to 18% lead to a rise in the LCOE for HES. This non-linear relationship underscores the importance of strategic financial planning to manage elevated financing costs and ensure the sustainability of renewable energy projects.

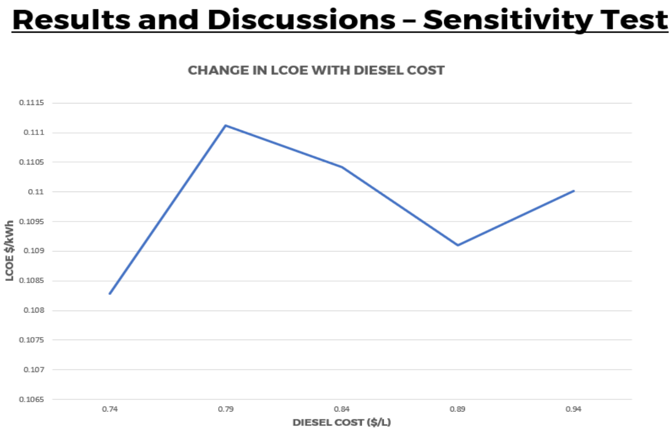

Figure 11 – Sensitivity with Diesel Cost

The sensitivity analysis of diesel costs on the LCOE for a HES as highlighted in *Figure* 11 shows a non-monotonic relationship, with LCOE peaking at $0.79/L before declining. This trend is influenced by the controller's logic, which shifts reliance to battery storage and renewable energy as diesel costs rise, highlighting the importance of smart energy management.

CONCLUSION

In summary, this study offers significant insights into optimizing HES for remote settlements by evaluating LF, CC and novel CS. Focused on Bambur village in Taraba State, Nigeria, the research highlights how different dispatch methods can influence system performance, cost efficiency, and sustainability.

The findings reveal that the Customized Strategy (CS) is the most practical and affordable choice, achieving the lowest NPC of $1,959,100 and a LCOE of $0.119/kWh, outperforming both the LF and CC. The CS strategy also showcased an optimal configuration of energy components, balancing the capacities of solar, wind, battery storage, and diesel generation to maximize energy production and reliability.

Local adaptation is necessary for HES, which prioritize RE and efficiency of the batteries. Because interest rates and diesel prices fluctuate, financial planning is essential. Performance is improved via customized dispatch, which prioritizes balanced energy integration over capacity maximization.

This study advances knowledge of sustainable energy options for remote populations by showing that enhanced HES can provide dependable, reasonably priced electricity to places without grid connectivity. The promising results of the Customized Strategy pave the way for future research into adaptive energy management systems, potentially leveraging machine learning for real-time decision-making.

As global efforts to address rural electrification and transition to sustainable energy continue, this study serves as a valuable resource for policymakers, engineers, and communities aiming to implement effective energy solutions. The findings not only provide a framework for enhancing energy access in Nigeria but also offer adaptable strategies for similar challenges faced worldwide.

REFERENCES

1. M. U. Emezirinwune, I. A. Adejumobi, O. I. Adebisi, and F. G. Akinboro, “Synergizing hybrid renewable energy systems and sustainable agriculture for rural development in Nigeria,” e-Prime - Advances in Electrical Engineering, Electronics and Energy, vol. 7, p. 100492, Mar. 2024, doi: 10.1016/j.prime.2024.100492.
2. Sk. A. Shezan et al., “Effective dispatch strategies assortment according to the effect of the operation for an islanded hybrid microgrid,” Energy Conversion and Management: X, vol. 14, p. 100192, May 2022, doi: 10.1016/j.ecmx.2022.100192.
3. A. O. Yakub, N. N. Same, A. B. Owolabi, B. E. K. Nsafon, D. Suh, and J. S. Huh, “Optimizing the performance of hybrid renewable energy systems to accelerate a sustainable energy transition in Nigeria: A case study of a rural healthcare centre in Kano,” Energy Strategy Reviews, vol. 43, Sep. 2022, doi: 10.1016/j.esr.2022.100906.
4. A. Aziz, M. Tajuddin, M. Adzman, M. Ramli, and S. Mekhilef, “Energy Management and Optimization of a PV/Diesel/Battery Hybrid Energy System Using a Combined Dispatch Strategy,” Sustainability, vol. 11, no. 3, p. 683, Jan. 2019, doi: 10.3390/su11030683.
5. A. Cano, P. Arévalo, and F. Jurado, “Energy analysis and techno-economic assessment of a hybrid PV/HKT/BAT system using biomass gasifier: Cuenca-Ecuador case study,” Energy, vol. 202, p. 117727, Jul. 2020, doi: 10.1016/j.energy.2020.117727.
6. M. Ramesh and R. P. Saini, “Dispatch strategies based performance analysis of a hybrid renewable energy system for a remote rural area in India,” J Clean Prod, vol. 259, p. 120697, Jun. 2020, doi: 10.1016/j.jclepro.2020.120697.
7. M. Amin Vaziri Rad, A. Shahsavari, F. Rajaee, A. Kasaeian, F. Pourfayaz, and W.-M. Yan, “Techno-economic assessment of a hybrid system for energy supply in the affected areas by natural disasters: A case study,” Energy Convers Manag, vol. 221, p. 113170, Oct. 2020, doi: 10.1016/j.enconman.2020.113170.
8. M. Ramesh and R. P. Saini, “Demand Side Management based techno-economic performance analysis for a stand-alone hybrid renewable energy system of India,” Energy Sources, Part A: Recovery, Utilization, and Environmental Effects, pp. 1–29, Jan. 2021, doi: 10.1080/15567036.2020.1851820.
9. SK. A. Shezan, S. S. Ali, and Z. Rahman, “Design and implementation of an islanded hybrid microgrid system for a large resort center for <scp>Penang Island</scp> with the proper application of excess energy,” Environ Prog Sustain Energy, vol. 40, no. 4, Jul. 2021, doi: 10.1002/ep.13584.
10. W. Chen, H. Ren, and W. Zhou, “Review of multi-objective optimization in long-term energy system models,” Global Energy Interconnection, vol. 6, no. 5, pp. 645–660, Oct. 2023, doi: 10.1016/j.gloei.2023.10.010.
11. S. I. Abba et al., “Emerging Harris Hawks Optimization based load demand forecasting and optimal sizing of stand-alone hybrid renewable energy systems– A case study of Kano and Abuja, Nigeria,” Results in Engineering, vol. 12, p. 100260, Dec. 2021, doi: 10.1016/j.rineng.2021.100260.
12. A. Toopshekan, H. Yousefi, and F. R. Astaraei, “Technical, economic, and performance analysis of a hybrid energy system using a novel dispatch strategy,” Energy, vol. 213, p. 118850, Dec. 2020, doi: 10.1016/j.energy.2020.118850.
13. L. Uwineza, H.-G. Kim, J. Kleissl, and C. K. Kim, “Technical Control and Optimal Dispatch Strategy for a Hybrid Energy System,” Energies (Basel), vol. 15, no. 8, p. 2744, Apr. 2022, doi: 10.3390/en15082744.
14. D. Zhao et al., “Capacity optimization and energy dispatch strategy of hybrid energy storage system based on proton exchange membrane electrolyzer cell,” Energy Convers Manag, vol. 272, p. 116366, Nov. 2022, doi: 10.1016/j.enconman.2022.116366.

ISSN No. 2321-2705 | DOI: 10.51244/IJRSI |Volume XI Issue VIII August 2024

15. Md. F. Ishraque, Sk. A. Shezan, J. N. Nur, and Md. S. Islam, “Optimal Sizing and Assessment of an Islanded Photovoltaic <scp>-Battery-</scp> Diesel Generator Microgrid Applicable to a Remote School of Bangladesh,” Engineering Reports, vol. 3, no. 1, Jan. 2021, doi: 10.1002/eng2.12281.
16. B. A. A. Yousef, R. Amjad, N. A. Alajmi, and H. Rezk, “Feasibility of integrated photovoltaic and mechanical storage systems for irrigation purposes in remote areas: Optimization, energy management, and multicriteria decision-making,” Case Studies in Thermal Engineering, vol. 38, p. 102363, Oct. 2022, doi: 10.1016/j.csite.2022.102363.
17. Y. B. Beyene, G. B. Worku, and L. B. Tjernberg, “On the design and optimization of distributed energy resources for sustainable grid-integrated microgrid in Ethiopia,” Int J Hydrogen Energy, vol. 48, no. 78, pp. 30282–30298, Sep. 2023, doi: 10.1016/j.ijhydene.2023.04.192.
18. S. A. Adetoro, L. Olatomiwa, J. Tsado, and S. M. Dauda, “A comparative analysis of the performance of multiple meta-heuristic algorithms in sizing hybrid energy systems connected to an unreliable grid,” e-Prime - Advances in Electrical Engineering, Electronics and Energy, vol. 4, p. 100140, Jun. 2023, doi: 10.1016/j.prime.2023.100140.
19. J. O. Oladigbolu, Y. A. Al-Turki, and L. Olatomiwa, “Comparative study and sensitivity analysis of a standalone hybrid energy system for electrification of rural healthcare facility in Nigeria,” Alexandria Engineering Journal, vol. 60, no. 6, pp. 5547–5565, Dec. 2021, doi: 10.1016/j.aej.2021.04.042.
20. S. Jamshidi, K. Pourhossein, and M. Asadi, “Size estimation of wind/solar hybrid renewable energy systems without detailed wind and irradiation data: A feasibility study,” Energy Convers Manag, vol. 234, p. 113905, Apr. 2021, doi: 10.1016/j.enconman.2021.113905.
21. H. A. El-Sattar, H. M. Sultan, S. Kamel, T. Khurshaid, and C. Rahmann, “Optimal design of stand-alone hybrid PV/wind/biomass/battery energy storage system in Abu-Monqar, Egypt,” J Energy Storage, vol. 44, p. 103336, Dec. 2021, doi: 10.1016/j.est.2021.103336.
22. S. A. Adetoro, M. Ndubuka Nwohu, and L. Olatomiwa, “Techno-economic Analysis of Hybrid Energy System Connected to an Unreliable Grid: A Case Study of a Rural Community in Nigeria,” in 2022 IEEE Nigeria 4th International Conference on Disruptive Technologies for Sustainable Development (NIGERCON), IEEE, Apr. 2022, pp. 1–5. doi: 10.1109/NIGERCON54645.2022.9803128.
23. H. Mohamed Ismail, H. K. Ng, S. Gan, and T. Lucchini, “Computational study of biodiesel–diesel fuel blends on emission characteristics for a light-duty diesel engine using Open FOAM,” Appl Energy, vol. 111, pp. 827–841, Nov. 2013, doi: 10.1016/j.apenergy.2013.05.068.